RSC Sustainability

ROYAL SOCIETY OF CHEMISTRY

TUTORIAL REVIEW

View Article Online
View Journal | View Issue

Cite this: *RSC Sustainability*, 2025, **3**, 5070

Synthesis and applications of carbon nano-onions and their composites for the remediation of organic pollutants from wastewater

Poonam Kumari,[ab] Anjali Chholak,[b] Kumud Malika Tripathi,[c] Kamlendra Awasthi *[d] and Ragini Gupta *[be]

Received 10th June 2025
Accepted 3rd September 2025

DOI: 10.1039/d5su00422e

rsc.li/rscsus

Water pollution remains a critical global concern, adversely impacting aquatic ecosystems, food security, and human health. In response, carbon nano-onions (CNOs) have emerged as promising nanomaterials for wastewater treatment due to their unique physicochemical properties, including high specific surface area, tunable surface chemistry, and multiple active sites. This review systematically explores recent advancements in the synthesis and functionalization of CNOs and their composites for the removal of organic pollutants from contaminated water. Key focus areas include adsorption capacities, photocatalytic degradation efficiencies, and reusability over multiple cycles with minimal performance loss. Mechanistic insights into pollutant–CNO interactions, including π–π stacking, electrostatic attraction, and redox reactions, are discussed in detail. Furthermore, challenges related to material regeneration, scalability, and real wastewater application are critically assessed. By consolidating current knowledge and outlining future research directions, this review aims to guide the rational design and deployment of CNO-based technologies for sustainable and high-performance water purification.

Sustainability spotlight

This review highlights the sustainable potential of carbon nano-onions (CNOs) and their composites for wastewater remediation. Emphasizing green synthesis strategies, high efficiency in pollutant removal, and reusability, the work underscores how CNO-based materials offer environmentally benign and scalable solutions for organic pollutant degradation. The study aligns with global goals for clean water and sustainable environmental technologies.

1. Introduction

The continuous rise in global population, environmental changes, urbanization, and industrial growth have significantly impacted water quality, leading to a growing freshwater crisis worldwide. Polluted water adversely affects aquatic life, the food chain, human health, and ecosystems. Consequently, the research community has shown great interest in developing methods to treat polluted water and ensure its long-term sustainability for the future.[1,2]

Water pollution is the introduction of excessive amounts of harmful substances into water, leading to its detrimental effects on humans, aquatic life, and the environment, or resulting in significant disruptions to the typical behaviours of various existing communities in or near water environments. Hence, water pollution disrupts the normal functioning of water-related activities, which encompass agriculture, public water supply, industries, and aquatic ecosystems. Water pollution is now a concern not only for public health but also for the conservation, aesthetics, and protection of natural resources. It signifies a deviation from the original state, resulting from changes that affect its functioning and characteristic properties. Any alteration in the naturally occurring dynamic balance among environmental components like the hydrosphere, atmosphere, lithosphere, or sediments can lead to the occurrence of water pollution.[3,4]

1.1 Sources of water pollution: impact on ecosystems and human health

Water pollution has emerged as one of the most pressing environmental challenges of the 21st century, fueled by rapid industrialization, urban expansion, and intensive agricultural activities. Although approximately 71% of the Earth's surface is

[a]*Department of Basic & Applied Science, Vivekananda Global University, Jaipur, Rajasthan 303012, India*

[b]*Department of Chemistry, Malaviya National Institute of Technology Jaipur, Rajasthan 302017, India. E-mail: rgupta.chy@mnit.ac.in*

[c]*Center for Emerging Technologies for Sustainable Development (CETSD), Indian Institute of Technology Jodhpur, Jodhpur, Rajasthan, 342030, India*

[d]*Department of Physics, Malaviya National Institute of Technology Jaipur, Rajasthan 302017, India. E-mail: kawasthi.phy@mnit.ac.in*

[e]*Materials Research Centre, Malaviya National Institute of Technology Jaipur, Rajasthan 302017, India*

Fig. 1 Sources of wastewater and their adverse effects.[12]

covered by water, only about 3% exists as freshwater, most of which is locked in ice and glaciers, leaving a small fraction available in liquid form in lakes, rivers, and groundwater.[3] This limited supply is increasingly threatened by a growing array of contaminants entering aquatic systems from multiple sources (Fig. 1). A major contributor to this crisis is the proliferation of emerging organic contaminants (EOCs), a diverse group of both well-known and newly developed chemicals with significant ecological and human health risks. These include pharmaceuticals, personal care products, pesticides, veterinary drugs, industrial byproducts, food additives, and engineered nanomaterials, hundreds of which have been detected globally in water bodies.[5,6] Their sources are varied, ranging from inadequately equipped WWTPs and hospital effluents to livestock waste, septic systems, and industrial discharges. Conventional treatment technologies often fail to effectively remove these persistent pollutants, allowing them to accumulate and exert long-term environmental impacts.[7,8]

The situation is further aggravated by large-scale industrial dye pollution. Industries such as textiles, pharmaceuticals, agriculture, leather, cosmetics, paints, and paper release significant volumes of synthetic dyes such as methyl orange (MO), crystal violet (CV), methylene blue (MB), Congo red (CR), methyl red, and rhodamine B (Rh B) into waterways. Global dye production approaches a million tons annually, with many dyes being toxic, highly persistent, and resistant to biodegradation. These pollutants can block light penetration and disrupt photosynthesis in aquatic plants, destabilize ecosystems, and cause severe human health problems, including kidney damage, skin disorders, cancer, allergic reactions, and mutagenic effects (Fig. 1).[9] Beyond dyes, a wide variety of other organic pollutants such as antibiotics, fertilizers, *p*-nitrophenol (PNP), 2,4-dinitrophenol (DNP), organohalides, and surfactants are extensively employed as intermediates in the production of chemicals, petrochemicals, wood stabilizers, pesticides, and pharmaceuticals. These substances are characterized by their widespread use, environmental persistence, high resistance to natural degradation, and potential to cause long-term ecological damage.[10,11]

In this context, wastewater must be considered a vital alternative water resource, and its safe and efficient reuse is essential to ensure sustainable water availability. The alarming trends in pollutant diversity, persistence, and toxicity highlight the urgent need for advanced, cost-effective, and sustainable water purification strategies to protect both environmental integrity and human well-being.

1.2 Overview of wastewater treatment methods

Organic dyes, metal ions, salts, phenolic compounds and pharmaceuticals are used as intermediates in a wide range of applications. However, discharge into the environment and improper handling are contaminating aquatic bodies, leading to hazardous and detrimental effects on our ecosystem, including humans. As a result, elimination of organic/inorganic contaminants from wastewater has proven to be a significant issue.[13] Numerous initiatives have been undertaken to eliminate and degrade organic contaminants from water. Organic/inorganic pollutants and their degradation products are removed and reduced from the aqueous system through physical, chemical, and biological techniques. Also, other techniques such as membrane filtration, adsorption, oxidation, electrochemical method and photocatalysis have been used for the elimination of pollutants from wastewater.[14,15] However, current wastewater treatment methods and materials still face several limitations regarding process sustainability, efficiency, recyclability, cost, energy consumption, and environmental impact.[16,17] For instance, advanced oxidation and membrane treatments are expensive, while bioremediation is constrained by its dependence on complex infrastructure and the necessity for sludge treatment. The coagulation and flocculation

processes face certain limitations and challenges. Inorganic coagulants generate high toxicity, posing risks to human health and the environment. Additionally, these coagulants produce large quantities of toxic sludge and are inefficient in the removal of emerging pollutants and heavy metal ions, and the complexity of the scaling up procedure is presented.[18] The photocatalysis technique is eco-friendly, safe, and sustainable for degrading organic pollutants. This technology eliminates organic pollutants from polluted water without producing harmful by-products, as the hazardous molecules are completely destroyed or converted into non-toxic forms. This process has limitations as it depends on environmental factors such as light intensity and temperature, which affect its feasibility.[19] Additionally, it presents challenges for large-scale industrial applications.

In this study, we thoroughly examined adsorption and photocatalytic methods for removing or reducing organic contaminants from wastewater. These approaches are widely recognized, cost-effective, and economically scalable.

A wide range of advanced nanomaterials including metal oxides, quantum dots, MOFs, and polymer-based composites have been explored for wastewater treatment due to their high surface area, enhanced reactivity, and tunable surface functionalities. However, among these, carbon-based nanomaterials have emerged as particularly promising candidates owing to their unique structural, chemical, and electronic properties.[20,21] These materials, such as graphene, carbon nanotubes (CNTs), CNOs, activated carbon, and carbon dots, offer several advantages in water purification applications. Their high specific surface area allows for efficient adsorption of pollutants, while their surface functionalities can be modified to target specific contaminants such as heavy metals, dyes, pharmaceuticals, and organic toxins. Additionally, carbon nanomaterials exhibit strong mechanical strength, thermal stability, and in some cases, photocatalytic activity, making them highly durable and effective under diverse environmental conditions.[22]

While the broader field of advanced nanomaterials continues to expand rapidly, this discussion will focus in detail on carbon-based nanomaterials, examining their synthesis strategies, mechanisms of pollutant removal, and application-specific performance in wastewater treatment. By highlighting recent advances and challenges, we aim to underscore their potential as sustainable and scalable solutions to the growing problem of water pollution.

The term "nanocarbon" is increasingly used to describe a wide variety of carbon materials with specific functional characteristics and nanoscale dimensions that mostly depend on their specific nanoscale features.[23] Nanocarbon structures are generally classified into two categories according to the predominant types of covalent bonds that attach their carbon atoms. The initial group includes graphitic nanostructures, primarily composed of densely packed sp^2 carbon atoms having a hexagonal honeycomb structure. Nevertheless, these structures may also incorporate sp^3 carbon atoms at defect locations. Various nanocarbon structures have been included in this group, like onion-like carbon (OLC), carbon nano-horns (CHNs), CNTs, graphene, graphene nanosheets, and carbon dots.[24,25] Another group of nanocarbon structures comprises a diverse proportion of sp^3 and sp^2 carbon atoms, containing combinations of graphitic and amorphous domains, or primarily composed of sp^3 carbon atoms.[26] Presently, within this category, nanodiamond stands as the sole acknowledged member. However, certain varieties of carbon dots possessing non-graphitic structures could also be regarded as part of this group. One distinguishing feature of these nanoforms is that, like CNTs and SWNHs, they do not originate from graphene monolayers or fragments. The nanoallotropes of carbon can also be categorized on the basis of their morphological attributes. The first group comprises carbon nanostructures that feature hollow internal spaces, which include fullerene, CHNs and CNTs. The empty spaces within these porous nanostructures can accommodate foreign molecules, atoms, metals, and other nanostructures. Sometimes, they can create

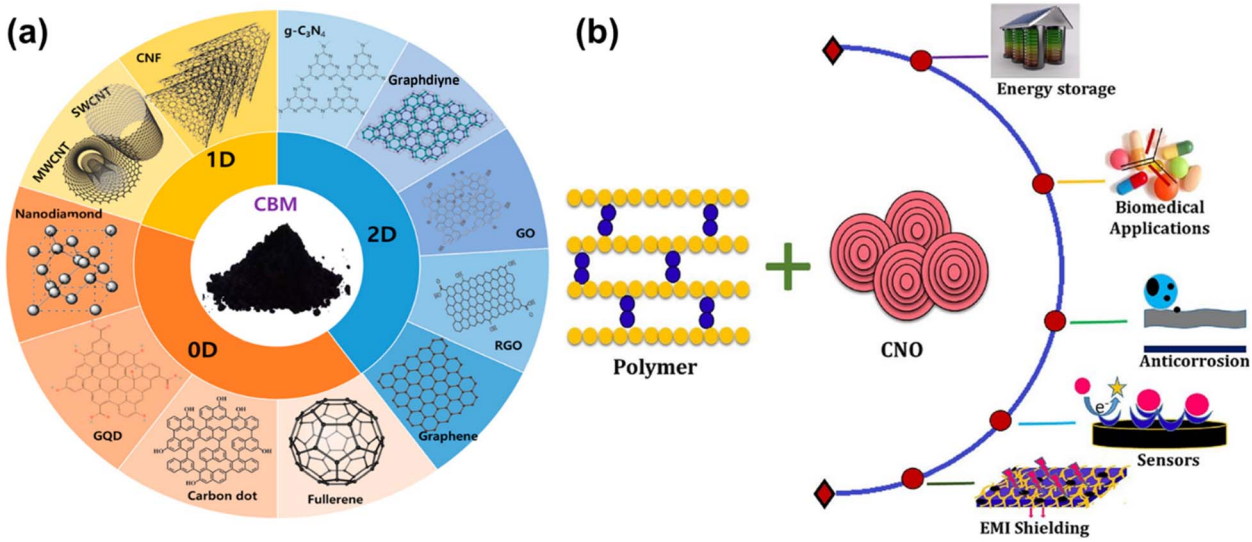

Fig. 2 (a) Schematic representation of various nanocarbons,[30] (b) application of CNO-based polymer composites in different fields.[33]

nanoenvironments conducive to particular reactions.[27] Durable nanostructures without internal voids, such as nanodiamonds, OLC spheres and C-dots would be categorized separately as the second group in this system. This group could also include graphene because it lacks internal spaces as well. Based on their dimensions, carbon nanostructures can also be categorized as: (i) 0D carbon nanoallotropes such as nanodiamonds, fullerene, CNOs, and C-dots, (ii) 1D carbon nanoallotropes such as CNTs, carbon nanofibers and SWNHs, and (iii) 2D nanoallotropes including few-layer graphene, graphene and nanoribbons.[28–30] A schematic representation of some nanocarbons is shown in Fig. 2(a). Nanocarbon materials find a variety of applications because of their unique combination of electrical and thermal conductivity, light weight, mechanical strength and biocompatible properties.[30,31] As a result, as shown in Fig. 2(b) a plethora of rapidly upsurging areas of research such as energy storage and generation, biomedicine, catalysts, plant growth, sensing of biomolecules and emerging pollutants, environmental remediation, and many others are rapidly advancing day by day.[32,33]

CNOs have recently become intriguing adsorbents due to their unique structure and chemical properties.[32] In recent years, various adsorption and photocatalytic degradation review studies of carbonaceous nanomaterials and their metal oxide composite have been reported for the removal of organic pollutants from wastewater.[30,34,35] However, compared to the extensive research on other nanocarbons and metal oxide composites used in adsorption and photocatalysis, there is limited study on CNOs and their composites specifically for organic pollutant removal. Therefore, this review focuses on CNOs and their composites for adsorbing and photodegrading organic pollutants.

2. Carbon nano-onions (CNOs)

In 1985, Curl, Kroto, and Smalley unveiled the groundbreaking carbon nanostructure fullerene (C60) through laser desorption experiments. Their pioneering discovery revolutionized chemistry and awarded them the Nobel Prize in 1996.[36,37] This discovery marked a noteworthy advancement in the field of materials chemistry at that particular time. The additional physicochemical analysis revealed certain attributes of these zero-dimensional nanostructures. These included exclusive electronic and structural characteristics, a high surface-area-to-volume ratio, their ability for reversible electron acceptance, and extensive absorption bands resulting from their extended π-system.[36] In 1992, during the HRTEM analysis of carbon soot, Ugarte observed an unusual twisting of carbon nanoparticles, which was similar to an onion-like structure.[38] These carbon nanostructures are known as CNOs because they have a multi-layered cage-within-a-cage shape that is spherical.[37,39,40] CNOs are a distinctive class of quasi-spherical nanocarbons featuring consecutive layers of graphene enveloping either a filled or hollow core morphologically in between fullerene and graphitic nanotubes.[41] The onion-like structure of CNOs is characterized by small graphitic sp^2 carbon domains with highly localized π-electrons and peripheral defects, manifested as dangling bonds.[42,43] As a result, CNOs have high specific surface area, chemical stability, mechanical strength and electrochemical properties, providing them with desirable features for a wide range of applications in different fields.[44,45] These CNOs were synthesized by an electric discharge method and their production yield was very low and also produced side products. The limited or very low yield of this substance hindered additional

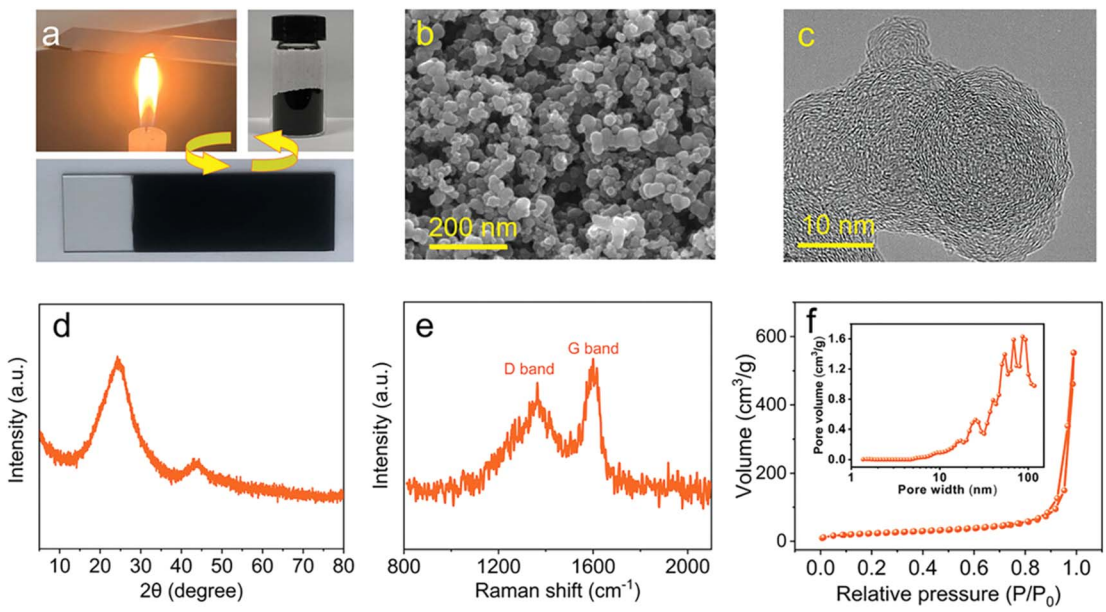

Fig. 3 (a) Schematic representation of the synthesis pathway for CNOs, (b) SEM micrograph revealing surface morphology, (c) high-resolution TEM image showcasing the layered onion-like carbon structure, (d) XRD profile confirming the graphitic crystalline structure; (e) Raman spectrum highlighting the structural order and defect density; (f) N_2 adsorption–desorption isotherm with inset pore size distribution, indicating textural properties.[47]

research into the characteristics of this newly discovered carbon variant.[46] Fig. 3(a) illustrates a rapid and straightforward synthesis of CNO powder *via* a combustion method. Fig. 3(b and c) shows SEM and TEM analyses reveal ~30–50 nm carbon nanoparticles with fused boundaries and imperfect onion-like graphitic layers, indicating edge defects. The XRD pattern in Fig. 3(d) confirms graphitic carbon phases with peaks at 24° and 43°, while the Raman spectrum in Fig. 3(e) shows a D/G intensity ratio of 0.89, highlighting structural disorder. The nitrogen adsorption isotherm shown in Fig. 3(f) demonstrates a meso/macroporous architecture with 0.855 $cm^3\ g^{-1}$ pore volume and 82 $m^2\ g^{-1}$ surface area.[47]

These carbonaceous materials are composed of a mixture of pentagonal and hexagonal rings.[48] In these structures, carbon atoms form two single bonds and one double bond with neighbouring carbon atoms, allowing the π-electron cloud to spread across the entire molecule. The graphitic layer of these nanostructures contains numerous voids and imperfections.[49] These spaces can be filled with pentagonal and heptagonal rings, leading to the formation of either non-crystalline or crystalline nanostructures.[50]

2.1 Synthesis methods of CNOs

To date, various methods for preparation of CNOs have been published. These methods include arc discharge,[51] chemical vapor deposition,[52] ion implantation,[53] flame pyrolysis,[54] annealing of nano-diamond[55] and microwave synthesis.[56] They can control and attain the desired onion size, shape, and structure based on their working and preparation factors. Reports on CNOs and their composite synthesis highlight their diverse applications.

2.1.1 Annealing of nano-diamond. Annealing of nano-diamond at high temperature in an inert environment under high vacuum was carried out according to Kuznetsov's method.[55] During the thermal annealing process, NDs start to convert into CNOs in a step-by-step process between 700 °C and 800 °C. In the initial phase, oxygen-containing groups are eliminated, resulting in the emission of carbon dioxide and carbon monoxide gases. The number of defects diminishes, and the outer graphene layers become more graphitic when the temperature ranges from 1100 °C to 1300 °C. Upon annealing NDs at temperatures up to 1800 °C, microscopic particles with few-layered graphitic shells emerge, giving rise to "small-scale" CNOs. When the NDs are heated to 1900 °C for the fourth step, polyhedral nanostructured onions are made. CNOs obtained from nanodiamonds by using thermal annealing have characteristic properties such as high electric conductivity and large surface area. During the thermal annealing process, the key properties like structure, specific surface area (SSA), morphology, and pore size distribution (PSD) of CNOs were altered. This was because nanodiamond acted as a synthesis parameter and as a result of physical activation in air. The SSA increased due to the elimination of surface impurities and functional groups. Oxidation in air is an effective method for removing predominantly amorphous carbon between the carbon onion particles and for stripping away the outer carbon shells.[57] Qiao *et al.* observed that small, irregular graphite fragments initially cover the surface of NDs. These fragments then connect with each other to eliminate dangling bonds, forming closed graphite shells,[58,59] shown in Fig. 4. Zeiger *et al.* synthesized CNOs in the presence of argon and an organic electrolyte (tetraethylammonium tetrafluoroborate in acetonitrile) resulting in highly interconnected few-layer graphene nanoribbons.[60] In another study, Feng *et al.* investigated the Compton profiles of nanodiamond-derived carbon onions using electron energy-loss spectroscopy in the electron

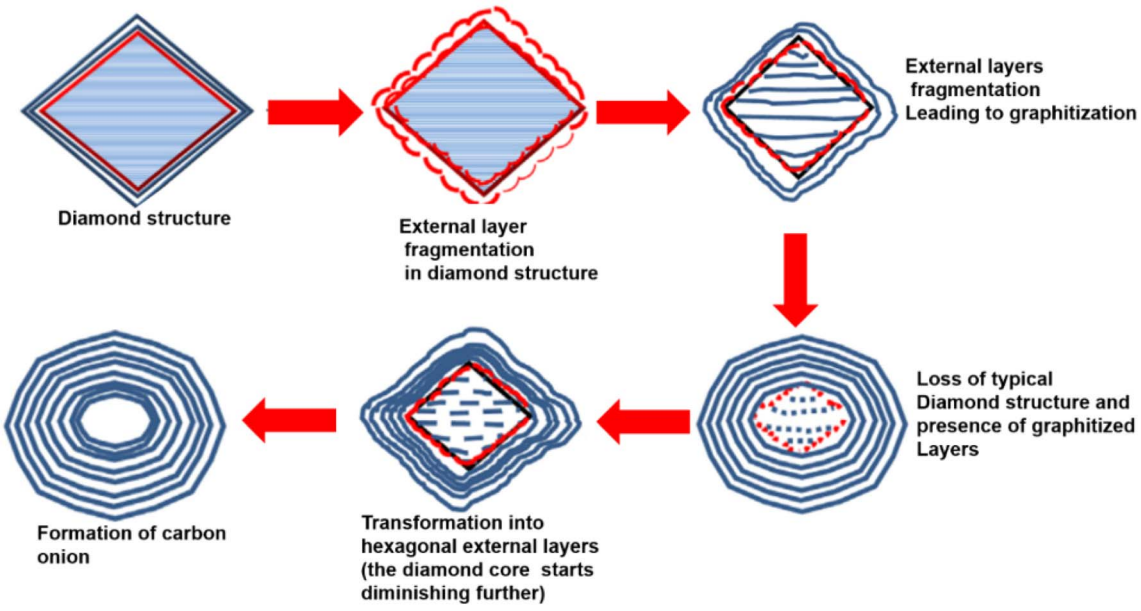

Fig. 4 Effect of increasing annealing temperature on the physicochemical properties of the as-formed CNOs from the detonation nanodiamond.[59]

Compton scattering region. The results indicated that as the annealing temperature exceeded 500 °C, the amplitude of the CPs at zero momentum increased. This suggested that graphitization likely occurs in this temperature range, with significant changes observed between 900 °C and 1300 °C. These findings demonstrated the thermal transformation of nanodiamond-derived CNOs and the enhancement of their electronic properties during the graphitization process.[61]

2.1.2 Chemical vapour deposition. Chemical vapour deposition (CVD) is the most applicable technique for the synthesis of CNOs because it is simple, and capable of controlling product growth and producing CNOs in gram scale quantity.[62] In this procedure CNOs were synthesized by a metal catalyst which exists at high pressure and temperature. Spherical CNOs ranging in size from 5 to 50 nm were obtained. Manawi *et al.* reviewed that during the CVD process, carbon atoms migrate through the heated molten substrate to produce CNOs.[63] In Fig. 5(a) the CNO growth mechanism by the CVD process is explained using the dissolve diffusion precipitation (DDP) model. Carbon moves through the metal catalyst, interacts with it, and dissolves into a metal carbide, which is the first seed. This confirms that in the CVD process, CNO formation started from 600 °C and it was found that there was uneven growth of onion rings. Upon increasing the temperature from 700 °C CNO rings formed properly and it was further proposed that due to low temperature a weak interaction occurred between the catalyst and copper support resulting in slowed down decomposition of methane gas. So, the effect of diffusion depends on the temperature and the concentration gradient. Upon further increasing the temperature, graphitic carbon layers completely cover the catalyst surface and completely convert into hollow CNOs because higher temperatures evaporate the catalyst particles.[59,63] In a research report on CNO synthesis, Ni–Fe catalyst powder was poured into a quartz boat and placed in a horizontal quartz tube furnace. The Fe–Ni catalyst was reduced at 400 °C and then different temperatures were used for the growth of CNOs at 750 °C, 850 °C and 950 °C for 1 h *via* using a highly pure mixture of CH_4 or N_2 at a particular flow rate and optimised suitable temperature for CNO synthesis. Finally, the obtained CNOs were cooled at room temperature in the presence of a N_2 atmosphere.[64] D. Medranda *et al.* reported a method in which, during the pyrolysis of ferrocene, sulphur was used in a small amount due to some characteristic reasons such as to control the diameter of CNOs, electrical and magnetic properties, structural morphology and number of shells.[65] Ruan *et al.* reported the fabrication *via* the CVD technique at 700 °C temperature with some advantages such as (i) possible coating of many components, (ii) sustained high temperature, (iii) very high deposition rate and obtainment of pure material, but during this process some byproducts were obtained which were hazardous and toxic.[52]

2.1.3 Arc discharge process. The arc discharge technique for the synthesis of CNOs will be elaborated in detail. A regulated environment, often made up of inert gases like argon or helium, is used in this procedure, where two graphite electrodes are placed close together. A plasma arc with an exceptionally high temperature is produced when a high-voltage electric discharge is started between the electrodes. Carbon atoms from the electrode surfaces are locally vaporised and sublimated by this extreme heat. As the plasma rapidly cools, the carbon atoms condense and aggregate quickly, resulting in the formation of spherical carbon nanostructures with numerous graphene layers. These layers are concentrically stacked, much like the layers of an onion. CNOs are then gathered and further processed as a result, as shown in Fig. 5(b). In a research study, CNOs were synthesized by an arc discharge method followed by such conditions, a bias potential of 16 V was applied and a 30 A constant current was required between the electrodes. As a result, lightweight CNOs were formed on the water surface and the size observed for these CNOs was in the range 15 to 25 nm.[66] Borgohain *et al.* synthesized activated CNOs; in this method pure graphite rods served as the anode and cathode. The synthesized A-CNOs were used in such areas as fuel-cell catalysis, energy-storage devices and biosensing and also showed good electrochemical properties such as accelerated electron-transfer kinetics with larger faradaic currents.[67] Furthermore, the high yield of CNOs was obtained by an arc-discharged method instead of other methods. During an experimental process the anode was allowed to rotate and the cathode was deposited in an underwater arc discharge between graphite electrodes after which the CNOs that were collected were highly pure, with size of 28 nm and structural order similar to graphitic planes.[68] A recent study described a composite graphite rod formed by mixing graphite with nickel powder, which was used as an anode, with a 50 × 50 mm graphite chunk serving as the cathode. During this process, an arc was

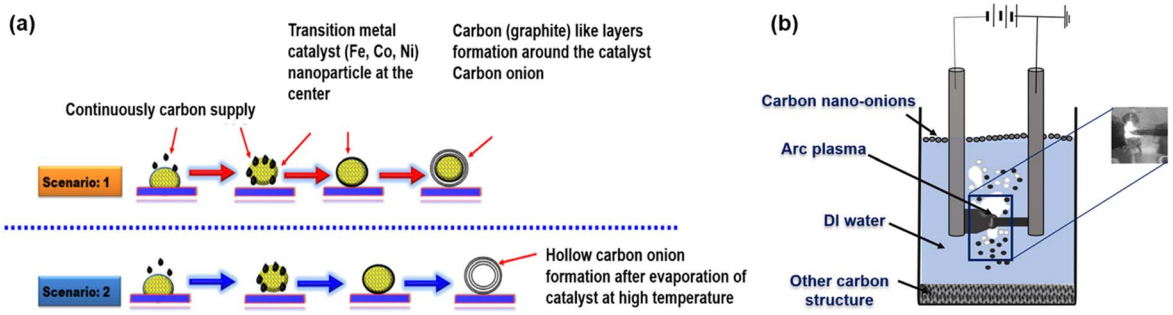

Fig. 5 (a) Step by step carbon nano-onion synthesis by the CVD process,[59] (b) synthesis of CNOs *via* the arc discharge process.[66]

Fig. 6 A schematic illustration for the synthesis of CNOs by the flame pyrolysis method.[77]

generated using a current of 110 A in a helium atmosphere at a pressure of 450 torr, with a 15 mm distance between the two electrodes. In another experiment, CNO composites synthesized using this method exhibited a higher heterogeneous electron transfer (HET) rate compared to hollow CNOs. They also demonstrated superior performance in applications such as supercapacitors and batteries.[69,70]

2.1.4 Flame pyrolysis method. Among the various reported strategies for the synthesis of CNOs, the conventional flame pyrolysis approach has gained remarkable attention in recent years owing to its cost-effectiveness, simplicity, versatility, eco-friendly nature, and scalability. This method involves the combustion of readily available carbon-rich precursors such as ghee,[71] waste frying oil,[72] flaxseed oil,[73] and candles, sometimes modified with metal additives like iron(III) acetylacetonate.[74] A key advantage of this process is the production of CNOs in high yield and purity, free from contamination with other carbon allotropes. Mohapatra and co-workers demonstrated the synthesis of OLCs by employing ghee as the precursor in a spirit lamp setup, where a cotton wick was partially submerged in ghee and ignited to generate a black flame. The soot deposited on a bronze plate was collected, yielding OLCs with a high surface area of 218 $m^2 g^{-1}$.[71] In another study, magnetic CNOs (MCNOs) were prepared by combusting a candle doped with iron(III) acetylacetonate, followed by annealing at 800 °C under nitrogen. These MCNOs exhibited excellent performance for the removal of bisphenol A (BPA) and other endocrine-disrupting compounds from wastewater.[75] Tripathi *et al.* further reported the synthesis of CNOs using flaxseed oil,[76] while Mohapatra *et al.* obtained ~30 nm sized CNOs by flame pyrolysis of ghee under low oxygen availability.[71] The morphology was found to depend strongly on the nature of the collecting substrate. Patel *et al.* (Fig. 6) and Kumari *et al.* synthesized CNOs using both waste frying oil and flaxseed oil *via* this method, further reinforcing the sustainability and waste-to-value aspect of flame pyrolysis.[77,78] Overall, the flame pyrolysis method stands out as one of the simplest, most economical, and environmentally benign routes for large-scale CNO synthesis, requiring neither sophisticated instrumentation nor catalytic assistance, thereby offering tremendous promise for sustainable nanocarbon production.[79]

3. Synthesis method of CNOs/composite nanomaterials

3.1 Sol–gel method

The sol–gel process is a versatile and widely adopted technique for the synthesis of advanced materials and composites, offering precise control over composition, morphology, and structural homogeneity. In this approach, a sol typically derived from metal alkoxides or related precursors is formed by dispersing molecular species or nanoparticles in a liquid medium, producing a stable colloidal suspension. Through hydrolysis and condensation reactions, the sol gradually evolves into a three-dimensional gel-like network. This gel can be further engineered by introducing polymers, organic molecules, or nanostructures (*e.g.*, carbon nanomaterials), thereby tailoring the final material properties. Due to its flexibility and cost-effectiveness, the sol–gel method is extensively employed for the synthesis of metal oxide nanostructures and their composites, particularly where enhanced mechanical, electrical, optical, or catalytic properties are desired.

Zhang *et al.* reported the fabrication of CNOs/TiO_2 composites. In their procedure, a solution of titanium isopropoxide ($C_{12}H_{28}O_4Ti$) in isopropanol was prepared and stirred at room temperature, followed by the addition of magnetic CNOs in varying proportions relative to TiO_2. The mixture was ultrasonicated, and subsequently added dropwise to deionized water, then stirred for 8 h at 80 °C before cooling, yielding well-dispersed CNOs/TiO_2 composites.[80] Building on this, the same group synthesized SiO_2/CNOs/TiO_2 ternary composites through a sequential sol–gel process. Initially, titanium isopropoxide was mixed with propanol and stirred, after which CNOs were introduced and nitric acid was carefully added dropwise at 80 °C to facilitate TiO_2 network formation. In the subsequent step, a silica sol was prepared separately and gradually incorporated into the CNOs/TiO_2 mixture under constant stirring. The resulting hybrid sol was dried at 100 °C, producing a SiO_2/CNOs/TiO_2 nanocomposite with enhanced structural integration. These examples highlight the remarkable adaptability of the sol–gel method for integrating CNOs with metal oxides, enabling the design of multifunctional nanocomposites with improved photocatalytic, electronic, and environmental remediation applications.[81]

3.2 Hydrothermal method

The hydrothermal method is a versatile and widely employed technique in materials science and chemistry for the synthesis of various materials, including crystals, nanoparticles, and ceramics. This process involves the controlled reaction of chemical precursors in an aqueous solution at elevated temperatures and pressures, typically within a specialized autoclave or reaction vessel. The term "hydrothermal" originates from the combination of "hydro" (water) and "thermal" (heat), highlighting the essential components of this method. By carefully manipulating factors such as temperature, pressure, reaction time, and precursor concentrations, researchers can tailor the properties and morphology of the resulting materials. The composite of CNOs was synthesized by many research groups. Weike Zhang *et al.* reported a Bi_2WO_6/MCNOs composite synthesized by using a hydrothermal method in which $Bi(NO_3)_3 \cdot 5H_2O$ was added to HNO_3 and mixed with $Na_2WO_4 \cdot 2H_2O$; the pH of this mixture was maintain between 2 and 3 by using NaOH solution; then MCNOs dispersed in

Table 1 Advantages and disadvantages of CNO synthesis processes

Synthesis method	Advantages	Limitations	References
Arc discharge	- High-quality CNOs with well-defined structures - Established technique	- Requires high temperature and an inert atmosphere - High energy consumption	66 and 67
Laser ablation	- Produces uniform and small-sized CNOs - High purity	- Expensive equipment - Limited scalability - High operational costs	86
Thermal annealing of nanodiamonds	- Simple method - Converts existing nanodiamond waste - Produces highly crystalline CNOs	- Requires high temperature (>1600 °C) - Limited precursor availability	58, 59 and 61
Chemical vapor deposition (CVD)	- Scalable - Controlled morphology and size - Tunable structure	- Requires metal catalysts - Complex setup - Expensive gaseous precursors	52, 62 and 64
Pyrolysis of organic precursors	- Cost-effective - Environmentally friendly - Can use biomass/waste	- Poor control over size and uniformity - May need post-purification steps	75
Flame synthesis	- Rapid and scalable - Inexpensive setup	- Poor control over morphology - Possibility of amorphous carbon contamination	72, 77 and 78
Electrochemical methods	- Room temperature synthesis - Tunable surface functional groups	- Low yield - Requires further processing - May involve hazardous reagents	87

ethane diol were mixed into the above solution and stirred for 30 min. After that the obtained mixture was transferred into an autoclave and heated at 150 °C for 2 h. After cooling, the sample was washed with ethanol many times. Finally, the obtained precipitate was dried at 80 °C for 8 h and theBi_2WO_6/MCNOs composite was obtained.[82] Recently reported nitrogen doped CNOs were synthesized by a hydrothermal method; in this process 1 g of *Lentinus edodes* powder was mixed into DI water and stirred for 20 min and after that dispersed by ultrasonication. In the above solution $Fe(NO_3)_3 \cdot 9H_2O$ was added and stirred for some time and the homogeneous solution was poured into an autoclave and heated 200 °C for 6 h. The obtained precipitate was washed and dried, and this powder was calcined at 300 °C under a nitrogen atmosphere. Excess iron oxide was removed using 0.1 M HCl solution; after that the sample was washed with DI water and ethanol many times and dried.[83]

3.3 Sonication method

Sonication is a highly effective method for the synthesis of CNT and carbon nanofiber (CNF) composites, offering precise control over the dispersion and integration of these nanomaterials. In this process, CNTs or CNFs are dispersed in a liquid medium, typically a solvent or a surfactant solution. The mixture is then subjected to ultrasonic waves, which create high-frequency mechanical vibrations. These vibrations lead to the formation of cavitation bubbles, causing localized heating and intense shear forces. As a result, the carbon nanotubes or nanofibers are exfoliated and uniformly dispersed within the liquid medium, facilitating their interaction with other materials or substrates. This sonochemical approach not only improves the homogeneity of the composite but also enhances its properties, making it a valuable technique in the synthesis of advanced materials with a wide range of applications, from reinforced polymers to high-performance composites in various industries. Lei Shi *et al.* synthesized an onion-like carbon porous g-C_3N_4 (OLC/pg-C_3N_4) composite. Firstly, OLC and porous g-C_3N_4 were added into 30 ml methanol and dispersed by ultrasonication followed by stirred at 80 °C until the solution was completely evaporated and heated at 300 °C for 60 min and finally the composite of OLC/pg-C_3N_4 was obtained.[84] Another T–ZnO–CNO composite was synthesized, in which CNOs were added into DI water and dispersed for 20 min to get a homogeneous solution. In the above solution T–ZnO was added and stirred for 12 h at room temperature. The obtained mixture was filtered and washed with DI water for removal of excess CNOs.[85] Table 1 presents a comparative overview of CNO synthesis methods, highlighting the key advantages and disadvantages of each reported technique.

4. Applications of CNOs and their composites

4.1 Adsorption

The term "adsorption" was coined by Heinrich Kayser (a German physicist) in 1881. According to IUPAC, this phenomenon is defined as "an increase in the concentration of a substance at the interface between a solid surface and a liquid or gaseous phase, attributed to surface forces," specifically the adhesion of atoms or molecules to a surface due to surface energy. The process of adsorption primarily involves surface atoms whose bonding capacity is not fully satisfied because they are not completely surrounded by other adsorbent particles, allowing them to attract the adsorbate.[88] The adsorption process has wide applications in wastewater treatment because it is simple, cheap and does not produce secondary pollutants

which is useful for elimination of inorganic and organic pollutants from wastewater. The adsorption process was investigated using different parameters such as concentration, temperature, solution pH and interaction forces between adsorbent and adsorbate.[89]

Adsorbents must possess a high surface area, suitable morphological properties, and robust chemical or mechanical stability to effectively remove organic pollutants from wastewater.[90] In aqueous environments, these contaminants act as adsorbates and adhere to the surfaces of adsorbents until an equilibrium is reached between the adsorbent and adsorbate. To study adsorption comprehensively, various types of adsorption isotherms, changes in Gibbs free energy, and entropy need to be thoroughly investigated. These characteristics are crucial for predicting adsorption performance and understanding its mechanism, which can involve chemical reactions, electrostatic interactions, repulsion, hydrogen bonding, van der Waals forces, and other factors.[91]

A simple adsorption isotherm (described by eqn (1)) measures the quantity of adsorbate absorbed based on temperature and adsorbent concentration.

$$q_t = \frac{(C_0 - C_t)V}{m} \quad (1)$$

where q_t (mg g^{-1}) represents the adsorption capacity at time t, V (L) is the volume of the solution, C_0 and C_t (mg L^{-1}) are the concentrations of the adsorbate initially and at time t, respectively, while m (g) is the mass of adsorbent.[92] However, this model was proposed without considering complex systems where many reaction parameters change simultaneously. The Freundlich isotherm, introduced in 1894, provided the best fit for gaseous adsorption but required several parameters.[93] In 1916, Irving Langmuir presented a model that became widely accepted, despite not accounting for all factors determining the adsorption rate. Thus, understanding the interaction between various adsorption parameters and the adsorption isotherm is crucial for obtaining useful information.[94] Gibbs free energy, along with entropy and enthalpy, provides insights into the spontaneity of a given reaction at a specific temperature. The Gibbs free energy of the adsorption process is related to the equilibrium constant by the Van't Hoff equation (eqn (2)).

$$\Delta G^0 = -RT \ln K_d \quad (2)$$

where ΔG^0 (kJ mol^{-1}) is the change in the Gibbs free energy, R is the universal gas constant, T (K) denotes the absolute temperature and K_d is the linear sorption distribution coefficient, which is expressed by eqn (3)

$$K_d = \frac{C_a}{C_e} \quad (3)$$

where C_a and C_e (mg L^{-1}) indicate the equilibrium adsorbate concentration on the adsorbent and equilibrium concentration in the solution, respectively.[95]

Zhou *et al.* reported on MCNOs that demonstrated effective adsorption of BPA,[75] as shown in Fig. 7(a). The adsorption capacity of the synthesized MCNOs was investigated at different temperatures: 700 °C, 800 °C, and 900 °C. It was found that the MCNOs synthesized at 800 °C exhibited the highest adsorption capacity for BPA removal, shown in Fig. 7(b). The differences in adsorption capacities among the MCNO samples can be attributed to variations in surface area, degree of graphitization, and the content of surface elements in the MCNOs produced at different temperatures. In another study, CNOs were synthesized using a simple wick and oil flame pyrolysis method with liquid paraffin. These synthesized CNOs were used in small quantities to remove MB from wastewater. As the initial concentration of the dye increases, the proportion of MB adsorbed decreases for all CNO samples. This occurs because the total accessible adsorption sites in the CNO adsorbents are limited, leading to a reduced removal rate of MB as the initial concentration increases. At an initial MB concentration of around 10 mg L^{-1}, nearly 93% of the MB is adsorbed from the solution, indicating that these CNOs could be effective adsorbents for wastewater treatment with low concentrations of MB using a small amount of adsorbent. It is confirmed that the surface of the CNOs is negatively charged. The zeta potential of CNOs decreases with increasing pH (from 2 to 12) due to the dissociation of the surface oxygen functions on the CNOs.[96] Gunture *et al.* reported water-soluble onion like carbon (wsONC) which was used for the removal of MB, CV, and Rh B dyes; among them higher removal efficiency was obtained for MB.[97] Kumari *et al.* reported the synthesis of CNOs using various oils, including waste frying oil, and demonstrated their application in the removal of antibiotics and pyridine from wastewater. The waste oil derived CNOs exhibited remarkable adsorption efficiency for antibiotics such as NOR and TCH, particularly under acidic conditions (pH 4), where the removal process was governed by π–π stacking interactions and hydrogen bonding. Notably, these CNOs maintained recyclability for up to five cycles with an efficiency retention of nearly 75%, highlighting their practical applicability.[78] In the case of pyridine removal, adsorption performance was strongly influenced by pH, with maximum efficiency observed at neutral pH (7). Beyond this point, a further increase in pH led to a decline in removal efficiency. Additionally, increasing pyridine concentration resulted in decreased removal efficiency but enhanced adsorption capacity, indicating efficient utilization of available active sites at higher pollutant loadings. Kinetic studies revealed that pyridine removal proceeded rapidly during the initial phase and attained equilibrium within 100 minutes, a behaviour attributed to the progressive saturation of adsorption sites on the CNO surface, shown in Fig. 7(c and d) respectively. The adsorption mechanism was primarily driven by π–π interactions between pyridine molecules and the conjugated carbon framework of CNOs, as shown in Fig. 7(e). The key attributes of these oil-derived CNOs namely their cost-effectiveness, sustainable production in gram-scale quantities, and recyclability underscore their strong potential for large-scale wastewater treatment applications.[73]

As illustrated in Fig. 8, Patel *et al.* demonstrated the synthesis of CNOs and proposed the adsorption mechanism of MB on their surface. The study revealed that MB adsorption is predominantly governed by a combination of electrostatic

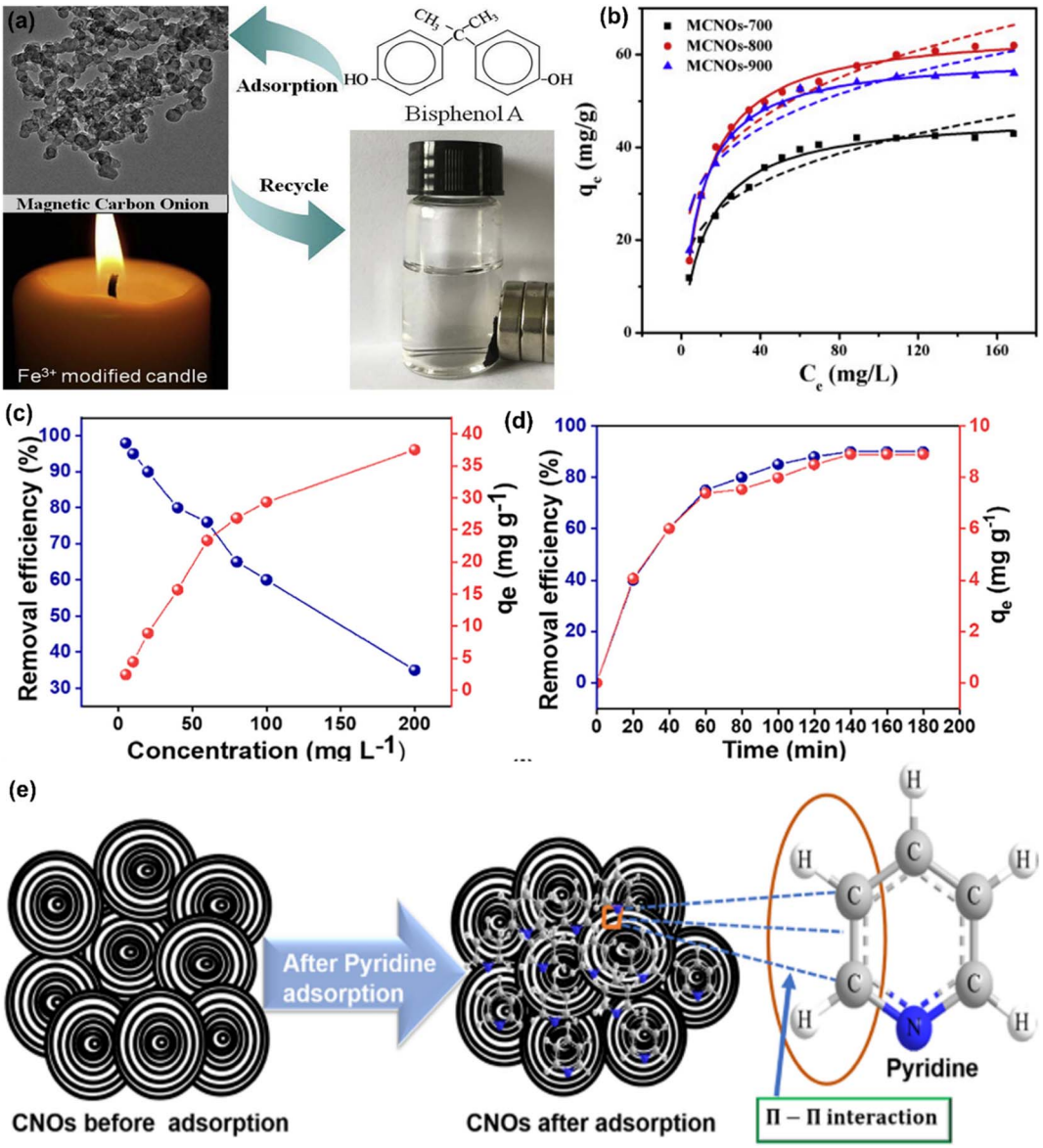

Fig. 7 (a) Magnetic nanocarbons showed adsorption of bisphenol A, (b) the adsorption capacity of MCNOs at different temperatures,[75] (c and d) removal efficiency of flax seed derived CNOs towards pyridine at different concentrations and times, (e) adsorption mechanism of pyridine on CNOs *via* π–π interaction.[73]

attractions, hydrogen bonding, and π–π stacking interactions between the dye molecules and the CNO framework. Moreover, the intrinsic surface defects of CNOs act as additional active sites, facilitating adsorption through π–π conjugation and other non-covalent interactions.[77]

4.2 Photocatalysis

Photocatalysis is a secure, sustainable, and environmentally beneficial approach for breaking down or degrading organic contaminants. This remediation approach offers an efficient means of eliminating organic contaminants from wastewater, ensuring that hazardous molecules are either completely degraded or transformed into environmentally benign by-products, thereby avoiding the generation of secondary pollutants.[98–100] In the photocatalytic process and reaction pathways depicted in Fig. 9(a and b), respectively, materials absorb photons with energies equal to or greater than the band gap energy between the photocatalyst's valence and conduction bands. This photon absorption initiates charge separation, and electrons are excited from the valence band to the conduction band, leaving behind positive holes in the valence band. In the conduction band, these positive holes oxidize water, generating hydroxyl radicals ($OH^{\bullet}$), while the excited electrons reduce adsorbed oxygen on the photocatalyst. The $OH^{\bullet}$ radicals subsequently attack the functional groups of organic pollutants, undergoing various processes to convert them into non-toxic substances or completely degrade them into CO_2 and H_2O.[101] The photocatalytic degradation efficiency of organic pollutants for wastewater remediation is governed by the kind and nature of organic pollutants, photocatalyst material, temperature and

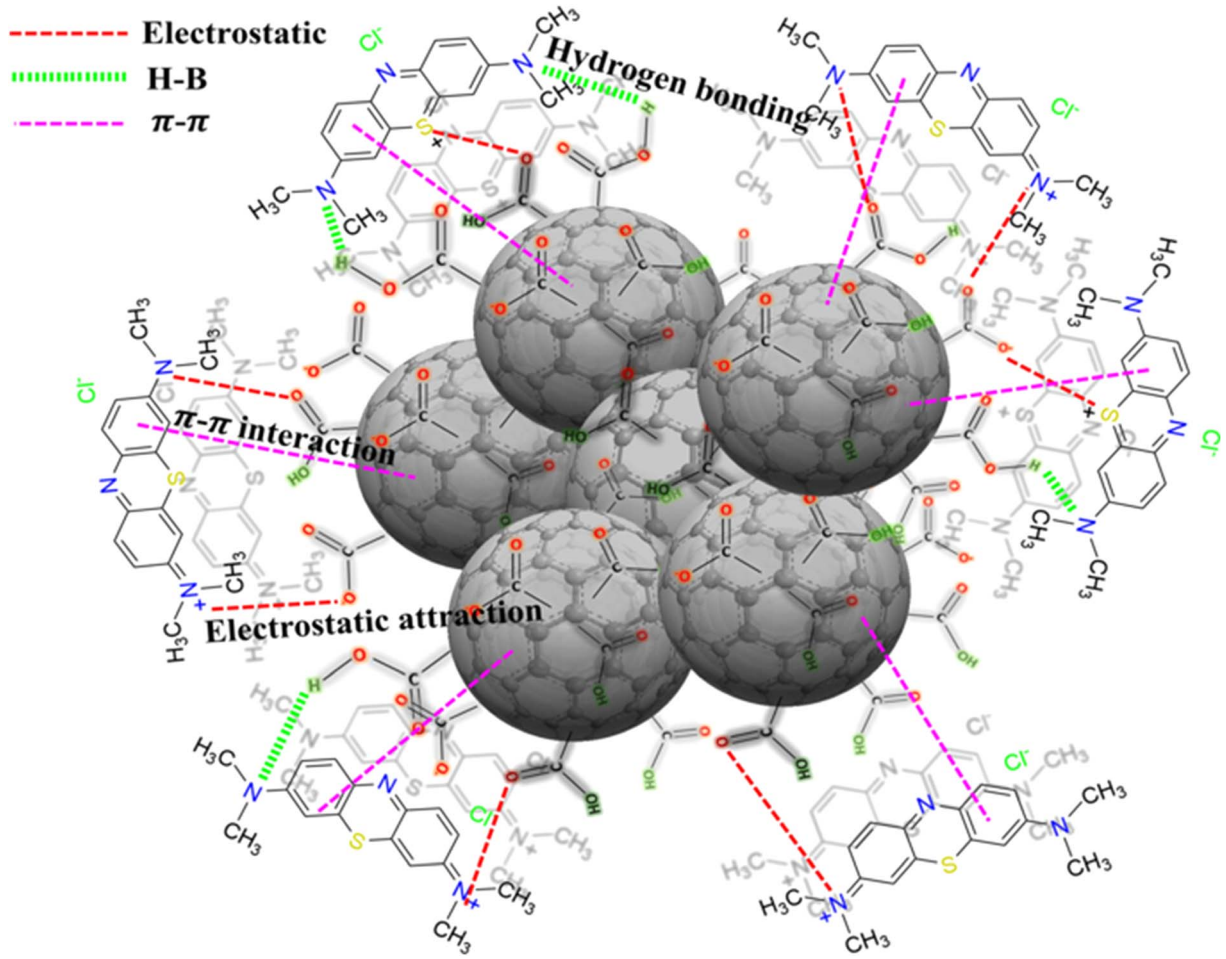

Fig. 8 A schematic illustration of methylene blue adsorption on CNOs.[77]

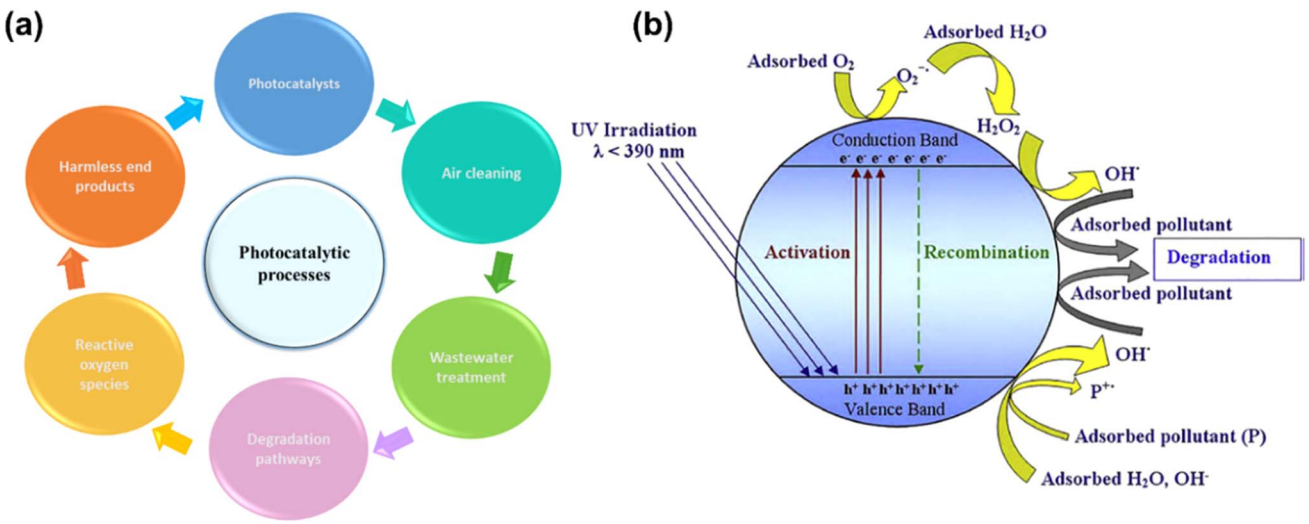

Fig. 9 Schematic demonstration of photocatalytic (a) process properties and (b) reaction pathways showing the degradation of organic pollutants *via* photogenerated electron–hole pairs.[103]

pH of the reaction medium, intensity of light, solvent type and other factors.[102] The chemical structure of organic pollutants and their associated functional groups also play a significant role in influencing photocatalytic processes. Typically, mono azo dyes degrade more rapidly under photodegradation conditions compared to anthraquinone dyes.[103]

CNOs enhance the photocatalytic degradation process when coupled with semiconductors such as TiO_2, ZnO, Bi_2WO_6, SiO_2 and g-C_3N_4 because, due to their high conductivity, they accept/transport photoelectrons, suppress electron/hole recombination and accelerate the formation of reactive oxygen species. The defects and π–π bonding in nitrogen, phosphorus and sulphur doped CNOs introduce mid-gap levels and sensitization effects, letting the composite harvest more of the solar spectrum and drive visible light reactions. For example, Zhang *et al.* prepared a composite of magnetically retrievable Bi_2WO_6/MCNOs by using the hydrothermal method which was used for environmental decontamination and showed the best photodegradation results towards several organic pollutants such as MB, RhB, MO, TC and PNP.[104,105]

For photocatalysis, SiO_2/CNOs/TiO_2 composites displayed excellent performance, with the 3% CNO-loaded sample achieving 96% degradation of RhB at an optimum dosage of 1.5 g L^{-1}. UV-visible spectra showed progressive reduction of the RhB absorption peak around 554 nm, accompanied by a blue shift (Fig. 10(a)) as the solution turned from pink to colorless within 150 min as depicted in Fig. 10(b).[81] Fig. 10(c) represents the photodegradation of RhB in the presence of different CNO composite ratios. Under dark conditions, all samples attained adsorption–desorption equilibrium within 30 min, with RhB adsorption efficiencies of ~35–45%, corresponding to 1.634–2.274 mg L^{-1}. This adsorption capacity was primarily attributed to the high surface area of SiO_2, which favors pollutant capture. Under light irradiation, the degradation efficiency of RhB was markedly enhanced in the presence of the prepared composites compared to the control without any photocatalyst. At lower CNO loadings (<3%), partial electron–hole recombination occurred, as photogenerated electrons

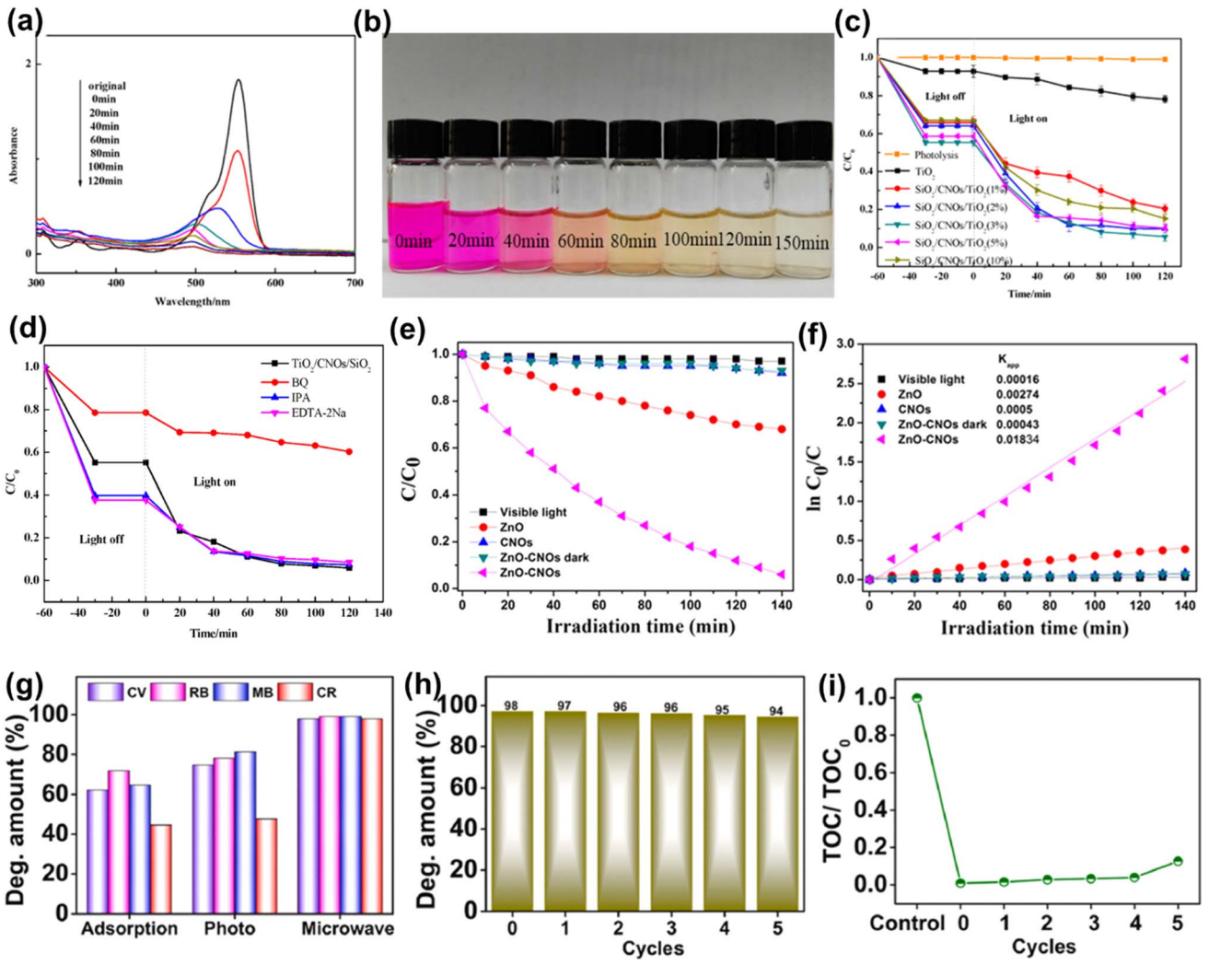

Fig. 10 (a) UV-vis spectra of RhB solution at different degradation times, (b) the color change of the RhB dye during photodegradation, (c) photocatalytic degradation with different CNO composite ratios, (d) reactive species trapping experiments of RhB with the SiO_2/CNOs/TiO_2 sample.[81] Visible-light-induced photodegradation of DNP with different photocatalysts, as a function of irradiation time, plotted as (e) (C/C_0) and (f) ln(C_0/C),[85] (g) comparison of dye degradation under optimized parameters under three different conditions: adsorption, photocatalytic and microwave degradation, (h) recycling study of microwave catalytic degradation of a mixture of dyes with CNOs, (i) TOC reduction during cyclic performance of CNOs.[106]

could not be efficiently transferred to CNOs. Conversely, excessive CNO content (>3%) promoted the formation of passivating layers, reducing both light absorption and the effective surface area of SiO_2/CNOs/TiO_2. The optimal performance was achieved at 3% CNO loading, where the composite exhibited the highest degradation efficiency of ~94%.[81] Radical scavenger experiments confirmed superoxide radicals ($O_2^{\bullet -}$) as the dominant species, since the addition of benzoquinone reduced the degradation efficiency from 94% to 60%, while isopropanol ($^{\bullet}OH$ scavenger) and EDTA-2Na (h^+ scavenger) had negligible impact (Fig. 10(d)).[81] Similarly, the T–ZnO–CNO hybrid composite exhibited superior photocatalytic degradation of DNP. Control experiments confirmed that neither direct photolysis nor individual CNOs or T–ZnO contributed significantly under visible light as shown in Fig. 10(e). In contrast, the composite achieved ~92% degradation, with the DNP absorption peak at 358 nm steadily decreasing without peak shifts or new band formation, indicating no chromophoric byproducts. The degradation rate constant of the hybrid was ~7 times higher than that of T–ZnO and ~36 times higher than that of CNOs alone (Fig. 10(f)).[85] Beyond photocatalysis, CNOs also demonstrated notable adsorption and microwave-assisted degradation of mixed dyes. Under dark conditions, adsorption efficiencies reached ~72% for RB and ~44% for CR, while under sunlight, removal reached ~81% for MB and ~47% for CR as demonstrated in Fig. 10(g).[106] Remarkably, microwave irradiation enabled nearly complete degradation (~98–99%) of CV, CR, RB, and MB within just 3 min (Fig. 10(g)).[106] The recyclability test result over five cycles shown in Fig. 10(h) confirms the sustained performance of CNOs, with ~94% degradation maintained. Total organic carbon (TOC) analysis (Fig. 10(i)) confirmed near-complete mineralization of dyes, with TOC decreasing from 8.11 mg L^{-1} to 0.07 mg L^{-1} after microwave treatment.[106] The slight TOC increase after recycling was attributed to minimal CNO loss during regeneration. These findings highlight the multifunctionality of CNOs as photocatalysts, and microwave-assisted degradants, where ROS generation (especially $O_2^{\bullet -}$), high conductivity, and structural stability synergistically drive efficient and sustainable wastewater treatment.[106]

CNOs serve as efficient co-catalysts by dispersing and anchoring semiconductor or metal nanoparticles (TiO_2, ZnO, Ag, *etc.*), thereby forming intimate heterojunctions (type-II, Z-scheme, or Schottky) that promote vectorial charge separation and radical generation. For instance, a CNO-functionalized ZnO composite (T–ZnO–CNO) demonstrated excellent photocatalytic performance, higher stability, and hydrophobicity. This hybrid degraded 2,4-dinitrophenol (DNP) up to 92% within 140 min. Interestingly, CNOs alone did not show catalytic activity nor adsorption of DNP, while pristine T–ZnO exhibited moderate photocatalysis under visible light without by-product formation, as evidenced by the absence of spectral peak shifts. The proposed Z-scheme pathway for DNP degradation is illustrated in Fig. 11(a),[85] with the corresponding reaction steps depicted in Fig. 11(b).[85] Under visible-light irradiation, CNOs become photoexcited and generate electron–hole pairs. The photogenerated electrons are transferred from CNOs to the conduction band of T–ZnO, where they react with adsorbed oxygen to produce $O_2^{\bullet -}$. Simultaneously, the holes are injected into the

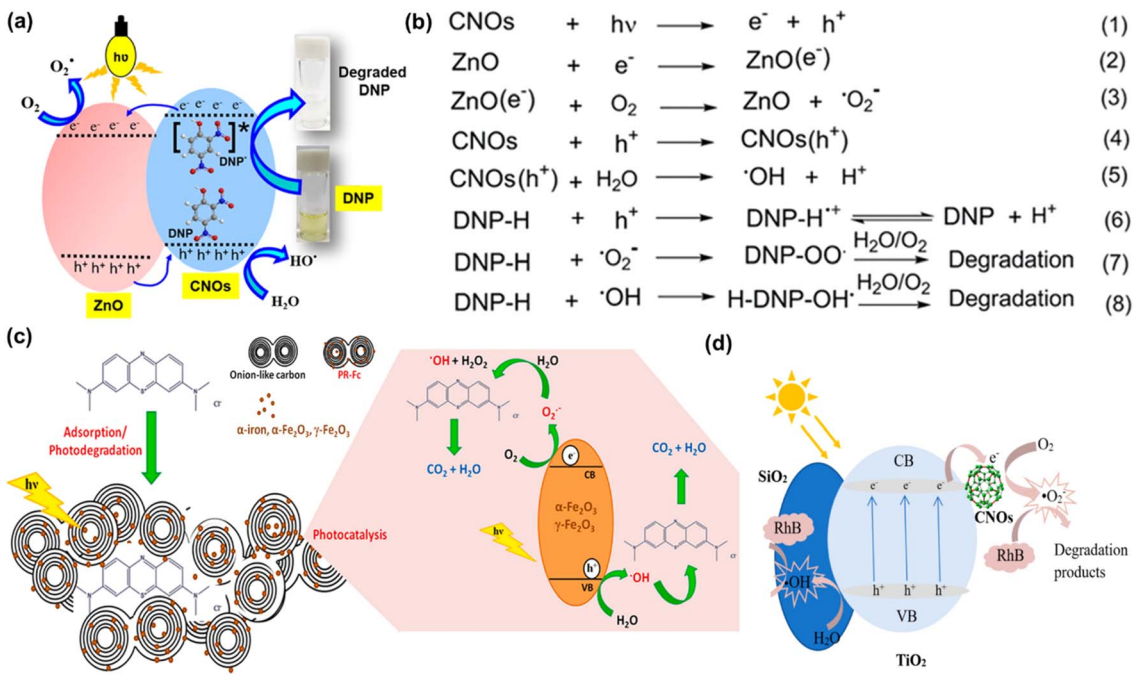

Fig. 11 (a) An illustration of the photodegradation of DNP by the T–ZnO–CNO hybrid composite, (b) a plausible mechanism of the photodegradation of DNP by the T–ZnO–CNO hybrid composite under visible-light irradiation,[85] (c) visual depiction of the synergistic adsorption–photocatalytic processes driving methylene blue degradation by the engineered PR-Fc catalyst,[107] (d) the mechanism diagram of SiO_2/CNOs/TiO_2 in the degradation of dyes in visible light.[81]

Table 2 Adsorption capacity (mg g^{-1}), removal efficiency (%), and degradation performance of carbon nano-onions (CNOs) and their composites

Material	Adsorbate	Method	pH	Time (min)	Capacity (mg g^{-1})/removal efficiency	Ref.
CNOs	MnO_4^-	Adsorption	7	70	806.45/99.9%	108
CNOs	Dichloromethane, aniline, toluene, diesel, methanol, ethanol, petrol, chloroform, and pyridine	Adsorption	6–7	160	90.95, 76 64, 58.1, 49.25, 42.25, 36.68, 36.25	73
CNOs	Nitrophenols	Adsorption	7	25	95%	109
CNOs	Tetracycline hydrochloride and norfloxacin	Adsorption	4	30–40	416.66 and 344.82/97% and 99%	78
CNOs	MO dye	Adsorption	6	30	166.66/99.95%	79
wsONC	MB, CV, and Rh B	Adsorption	7	60	247.78/—	110
CNOs	MB dye	Adsorption	7	10	1397.35/97.92%	96
CNOs	Red dye	Adsorption	7	120	85%	111
MCNOs	Bisphenol A	Adsorption	6	90	65.77	75
CNOs	Cr(VI)	Adsorption	3.4	1440	82%	112
NC materials	Phenol	Adsorption and degradation		360	56.28%	113
N,P-CNOs	MB dye	Degradation	—	120	75.8%	114
TiO_2/OLNC	MO	Degradation	7	120	99.9%	115
γ-Fe_2O_3	MB dye	Degradation	7	60	97%	82
Bi_2WO_6/MCNOs	Tetracycline and *p*-nitrophenol	Degradation	—	40	81.9% and 86.1%	116

valence band of CNOs, which oxidize water molecules to yield hydroxyl radicals (•OH). Among the reactive oxygen species, $O_2^{\bullet-}$ plays the dominant role in driving the photocatalytic degradation of DNP.[85] A dual mechanism of adsorption–photocatalysis was reported for PR-Fc catalysts featuring onion-like activated carbon and iron oxides. Here, high surface area and abundant active sites enabled strong adsorption of MB, with 97% dye removal achieved in 60 min. Adsorption occurred even without light exposure, while under illumination, Fe_2O_3 photoexcitation coupled with the conductive carbon matrix enhanced charge separation and ROS production, leading to rapid MB degradation as demonstrated in Fig. 11(c).[107] Furthermore, SiO_2/CNOs/TiO_2 composites displayed 96% degradation of RhB under UV-visible light, attributed to enhanced quantum efficiency of TiO_2. The excellent conductivity of CNOs facilitates the transfer of photogenerated electrons from the composite to molecular oxygen, generating $O_2^{\bullet-}$, which acts as the primary reactive species and effectively suppresses electron–hole recombination (Fig. 11(d)). In addition, the high surface concentration of Ti–O–Si linkages at the TiO_2/SiO_2 interface improves catalyst dispersion, thereby markedly enhancing the photocatalytic degradation efficiency of RhB.[81] Additionally, onion-like carbon modified porous g-C_3N_4 composites effectively degraded phenol and dyes under visible-light irradiation, underscoring the versatility of CNO-based hybrids in wastewater remediation.[58] Table 2 shows a comparison of performance metrics for CNOs and their composites.

5. Conclusion

This review offers a comprehensive exploration of the synthesis strategies and functional applications of CNOs and their composites, with a particular focus on their role in the removal of organic contaminants from wastewater through adsorption and photocatalytic techniques. Owing to their exceptional surface area, tunable surface chemistry, and rapid interaction kinetics, CNO-based materials have emerged as highly promising candidates for efficient water purification, even at trace pollutant levels. In adsorption-driven processes, the interfacial characteristics and structural morphology of the adsorbents are crucial for enhanced contaminant capture. Meanwhile, in photocatalytic systems, parameters such as charge carrier dynamics, radical generation efficiency, and light harvesting capabilities govern the degradation performance. The review also encapsulates recent innovations in the fabrication of CNOs, shedding light on current challenges and future directions for their environmental deployment.

Future research on CNO-based systems for wastewater treatment should emphasize their recyclability and reusability, which not only enhance cost-effectiveness but also promote environmental sustainability by minimizing secondary pollution and toxic waste. However, the generation and accumulation of secondary debris during treatment remain underexplored, posing potential risks to long-term ecological health. Addressing these concerns through greener synthesis approaches and responsible application frameworks will be crucial. Key directions include developing hybrid CNO-based materials by integrating metals, metal oxides, or polymers to enhance multifunctionality, employing advanced surface functionalization strategies to improve contaminant selectivity, and exploring green, scalable synthesis routes for cost-effective production. Additionally, pilot-scale studies using real wastewater and comprehensive assessments of long-term stability and regeneration are essential to ensure sustainable and practical deployment.

Conflicts of interest

There are no conflicts to declare.

Data availability

No new data were created or analyzed in this study. Data sharing is not applicable to this article. The sources are already acknowledged, and prior permission has been taken.

Notes and references

1 R. C. Bicho, F. C. F. Santos, J. J. Scott-Fordsmand and M. J. B. Amorim, Multigenerational effects of copper nanomaterials (CuONMs) are different of those of CuCl2: exposure in the soil invertebrate Enchytraeus crypticus, *Sci. Rep.*, 2017, **7**(1), 8457.

2 H. Dan, Y. Song, Y. Xu, Y. Gao, W. Kong, Y. Huang, Q. Yue and B. Gao, Green synthesis of Cu nanoparticles supported on straw-graphene composite for catalytic reduction of p-nitrophenol, *J. Clean. Prod.*, 2021, **283**, 124578.

3 R. Gusain, K. Gupta, P. Joshi and O. P. Khatri, Adsorptive removal and photocatalytic degradation of organic pollutants using metal oxides and their composites: a comprehensive review, *Adv. Colloid Interface Sci.*, 2019, **272**, 102009.

4 S. Madhav, A. Ahamad, A. K. Singh, J. Kushawaha, J. S. Chauhan, S. Sharma and P. Singh, Water Pollutants: Sources and Impact on the Environment and Human Health, in *Sensors in Water Pollutants Monitoring: Role of Material*, Springer, Singapore, 2020, pp. 43–62.

5 V. Matamoros, R. Gutiérrez, I. Ferrer, J. García and J. M. Bayona, Capability of microalgae-based wastewater treatment systems to remove emerging organic contaminants: a pilot-scale study, *J. Hazard. Mater.*, 2015, **288**, 34–42.

6 A. Saravanan, P. Thamarai, V. C. Deivayanai, S. Karishma, A. Shaji and P. R. Yaashikaa, Current strategies on bioremediation of personal care products and detergents: sustainability and life cycle assessment, *Chemosphere*, 2024, **354**, 141698.

7 T.-M. Scott, P. J. Phillips, D. W. Kolpin, K. M. Colella, E. T. Furlong, W. T. Foreman and J. L. Gray, Pharmaceutical manufacturing facility discharges can substantially increase the pharmaceutical load to U.S. wastewaters, *Sci. Total Environ.*, 2018, **636**, 69–79.

8 B. K. Navina, N. K. Velmurugan, P. Senthil Kumar, G. Rangasamy, J. Palanivelu, P. Thamarai, A. S. Vickram, A. Saravanan and A. Shakoor, Fungal bioremediation approaches for the removal of toxic pollutants: mechanistic understanding for biorefinery applications, *Chemosphere*, 2024, **350**, 141123.

9 S. Karimifard and M. R. Alavi Moghaddam, Application of response surface methodology in physicochemical removal of dyes from wastewater: a critical review, *Sci. Total Environ.*, 2018, **640–641**, 772–797.

10 E. V. Lau, S. Gan, H. K. Ng and P. E. Poh, Extraction agents for the removal of polycyclic aromatic hydrocarbons (PAHs) from soil in soil washing technologies, *Environ. Pollut.*, 2014, **184**, 640–649.

11 P. R. Yaashikaa, S. Karishma, R. Kamalesh, A. S. Vickram and K. Anbarasu, A systematic review on enhancement strategies in biochar-based remediation of polycyclic aromatic hydrocarbons, *Chemosphere*, 2024, **355**, 141796.

12 A. P. Periyasamy, Recent Advances in the Remediation of Textile-Dye-Containing Wastewater: Prioritizing Human Health and Sustainable Wastewater Treatment, *Sustainability*, 2024, **16**(2), 495.

13 R. Ahmad and I. Hasan, Efficient Remediation of an Aquatic Environment Contaminated by Cr(VI) and 2,4-Dinitrophenol by XG-g-Polyaniline@ZnO Nanocomposite, *J. Chem. Eng. Data*, 2017, **62**(5), 1594–1607.

14 N. Madima, S. B. Mishra, I. Inamuddin and A. K. Mishra, Carbon-based nanomaterials for remediation of organic and inorganic pollutants from wastewater. A review, *Environ. Chem. Lett.*, 2020, **18**(4), 1169–1191.

15 P. Kumari, K. M. Tripathi, L. K. Jangir, R. Gupta and K. Awasthi, Recent advances in application of the graphene-based membrane for water purification, *Mater. Today Chem.*, 2021, **22**, 100597.

16 X. Cao, Y. Oda and F. Shiraishi, Photocatalytic and adsorptive treatment of 2,4-dinitrophenol using a TiO2 film covering activated carbon surface, *Chem. Eng. J.*, 2010, **156**(1), 98–105.

17 P. Swaminaathan, A. Shaji, A. Saravanan and P. R. Yaashikaa, Innovative Approaches in Extremophile-Mediated Remediation of Toxic Pollutants: A Comprehensive Review, *Water Conserv. Sci. Eng.*, 2024, **9**(2), 39.

18 C. Y. Teh, P. M. Budiman, K. P. Y. Shak and T. Y. Wu, Recent Advancement of Coagulation–Flocculation and Its Application in Wastewater Treatment, *Ind. Eng. Chem. Res.*, 2016, **55**(16), 4363–4389.

19 M. N. Chong, B. Jin, C. W. K. Chow and C. Saint, Recent developments in photocatalytic water treatment technology: a review, *Water Res.*, 2010, **44**(10), 2997–3027.

20 S. Dey, K. Manna, P. Pradhan, A. N. Sarkar, A. Roy and S. Pal, Review of Polymeric Nanocomposites for Photocatalytic Wastewater Treatment, *ACS Appl. Nano Mater.*, 2024, **7**(5), 4588–4614.

21 H. Kaur, N. Devi, S. S. Siwal, W. F. Alsanie, M. K. Thakur and V. K. Thakur, Metal–Organic Framework-Based Materials for Wastewater Treatment: Superior Adsorbent Materials for the Removal of Hazardous Pollutants, *ACS Omega*, 2023, **8**(10), 9004–9030.

22 S. C. Smith and D. F. Rodrigues, Carbon-based nanomaterials for removal of chemical and biological contaminants from water: a review of mechanisms and applications, *Carbon*, 2015, **91**, 122–143.

23 D. S. Su, S. Perathoner and G. Centi, Nanocarbons for the Development of Advanced Catalysts, *Chem. Rev.*, 2013, **113**(8), 5782–5816.

24 T. N. Hoheisel, S. Schrettl, R. Szilluweit and H. Frauenrath, Nanostructured Carbonaceous Materials from Molecular Precursors, *Angew. Chem., Int. Ed. Engl.*, 2010, **49**(37), 6496–6515.
25 J. H. Bitter, Nanostructured carbons in catalysis a Janus material—industrial applicability and fundamental insights, *J. Mater. Chem.*, 2010, **20**(35), 7312–7321.
26 A. A. Balandin, Thermal properties of graphene and nanostructured carbon materials, *Nat. Mater.*, 2011, **10**(8), 569–581.
27 X. J. Lee, B. Y. Z. Hiew, K. C. Lai, L. Y. Lee, S. Gan, S. Thangalazhy-Gopakumar and S. Rigby, Review on graphene and its derivatives: synthesis methods and potential industrial implementation, *J. Taiwan Inst. Chem. Eng*, 2019, **98**, 163–180.
28 V. Georgakilas, J. A. Perman, J. Tucek and R. Zboril, Broad Family of Carbon Nanoallotropes: Classification, Chemistry, and Applications of Fullerenes, Carbon Dots, Nanotubes, Graphene, Nanodiamonds, and Combined Superstructures, *Chem. Rev.*, 2015, **115**(11), 4744–4822.
29 A. K. Geim and K. S. Novoselov, The rise of graphene, *Nat. Mater.*, 2007, **6**(3), 183–191.
30 L. Mohapatra, D. Cheon and S. H. Yoo, Carbon-Based Nanomaterials for Catalytic Wastewater Treatment: A Review, *Molecules*, 2023, **28**(4), 1805.
31 Q. Wu, L. Yang, X. Wang and Z. Hu, From Carbon-Based Nanotubes to Nanocages for Advanced Energy Conversion and Storage, *Acc. Chem. Res.*, 2017, **50**(2), 435–444.
32 A. Kausar and E. Ghavanloo, Carbon nano-onions reinforced nanocomposites: fabrication, computational modeling techniques and mechanical properties, *Crit. Rev. Solid State Mater. Sci.*, 2024, **49**(6), 1179–1201.
33 A. Vindhyasarumi, K. P. Anjali, A. S. Sethulekshmi, J. S. Jayan, B. D. S. Deeraj, A. Saritha and K. Joseph, A comprehensive review on recent progress in carbon nano-onion based polymer nanocomposites, *Eur. Polym. J.*, 2023, **194**, 112143.
34 V. I. Isaeva, M. D. Vedenyapina, A. Y. Kurmysheva, D. Weichgrebe, R. R. Nair, N. P. Nguyen and L. M. Kustov, Modern Carbon–Based Materials for Adsorptive Removal of Organic and Inorganic Pollutants from Water and Wastewater, *Molecules*, 2021, **26**(21), 6628.
35 M. M. Sabzehmeidani, S. Mahnaee, M. Ghaedi, H. Heidari and V. A. L. Roy, Carbon based materials: a review of adsorbents for inorganic and organic compounds, *Mater. Adv.*, 2021, **2**(2), 598–627.
36 M. E. Plonska-Brzezinska, Carbon Nano-Onions: A Review of Recent Progress in Synthesis and Applications, *ChemNanoMat*, 2019, **5**(5), 568–580.
37 C. M. Lieber and C.-C. Chen, Preparation of Fullerenes and Fullerene-Based Materials, in *Solid State Physics*, ed. H. Ehrenreich and F. Spaepen, Academic Press, 1994, vol. 48, pp. 109–148.
38 D. Ugarte, Curling and closure of graphitic networks under electron-beam irradiation, *Nature*, 1992, **359**, 707–709.
39 X. Liu, S. W. Or, C. Jin, Y. Lv, W. Li, C. Feng, F. Xiao and Y. Sun, Co3O4/C nanocapsules with onion-like carbon shells as anode material for lithium ion batteries, *Electrochim. Acta*, 2013, **100**, 140–146.
40 J. Bartelmess, S. J. Quinn and S. Giordani, Carbon nanomaterials: multi-functional agents for biomedical fluorescence and Raman imaging, *Chem. Soc. Rev.*, 2015, **44**(14), 4672–4698.
41 M. E. Plonska-Brzezinska, D. M. Brus, A. Molina-Ontoria and L. Echegoyen, Synthesis of carbon nano-onion and nickel hydroxide/oxide composites as supercapacitor electrodes, *RSC Adv.*, 2013, **3**(48), 25891–25901.
42 M. E. Plonska-Brzezinska and L. Echegoyen, Carbon nano-onions for supercapacitor electrodes: recent developments and applications, *J. Mater. Chem. A*, 2013, **1**(44), 13703–13714.
43 J. Bartelmess and S. Giordani, Carbon nano-onions (multi-layer fullerenes): chemistry and applications, *Beilstein J. Nanotechnol.*, 2014, **5**, 1980–1998.
44 J. Ahlawat, S. Masoudi Asil, G. Guillama Barroso, M. Nurunnabi and M. Narayan, Application of carbon nano onions in the biomedical field: recent advances and challenges, *Biomater. Sci.*, 2021, **9**(3), 626–644.
45 M. Zeiger, N. Jäckel, V. N. Mochalin and V. Presser, Review: carbon onions for electrochemical energy storage, *J. Mater. Chem. A*, 2016, **4**(9), 3172–3196.
46 J. P. Bartolome, L. Echegoyen and A. Fragoso, Reactive Carbon Nano-Onion Modified Glassy Carbon Surfaces as DNA Sensors for Human Papillomavirus Oncogene Detection with Enhanced Sensitivity, *Anal. Chem.*, 2015, **87**(13), 6744–6751.
47 X. Peng, Y. Li, F. Kang, X. Li, Z. Zheng and L. Dong, Negatively Charged Hydrophobic Carbon Nano-Onion Interfacial Layer Enabling High-Rate and Ultralong-Life Zn-Based Energy Storage, *Small*, 2024, **20**(4), 2305547.
48 R. Bacon, Growth, Structure, and Properties of Graphite Whiskers, *J. Appl. Phys.*, 1960, **31**(2), 283–290.
49 A. Camisasca and S. Giordani, Carbon Nano-onions for Bioimaging and Cancer Therapy Applications, in *Nanooncology: Engineering Nanomaterials for Cancer Therapy and Diagnosis*, ed. G. Gonçalves and G. Tobias, Springer International Publishing, Cham, 2018, pp. 417–455.
50 C. J. Brabec, A. Maiti and J. Bernholc, Structural defects and the shape of large fullerenes, *Chem. Phys. Lett.*, 1994, **219**(5), 473–478.
51 N. Sano, H. Wang, I. Alexandrou, M. Chhowalla, K. B. K. Teo, G. A. J. Amaratunga and K. Iimura, Properties of carbon onions produced by an arc discharge in water, *J. Appl. Phys.*, 2002, **92**(5), 2783–2788.
52 C. Ruan, Z. Li, D. Zhang, X. Yuan, C. Liang, Y. Chang, H. Huang, L. Xu and M. Chen, A scalable chemical vapor deposition synthesis of high purity hollow carbon onions, *Carbon*, 2020, **161**, 622–628.
53 E. Thune, T. Cabioc'h, P. Guérin, M. F. Denanot and M. Jaouen, Nucleation and growth of carbon onions synthesized by ion-implantation: a transmission electron microscopy study, *Mater. Lett.*, 2002, **54**(2), 222–228.

54 S. Jung, Y. Myung, G. S. Das, A. Bhatnagar, J.-W. Park, K. M. Tripathi and T. Kim, Carbon nano-onions from waste oil for application in energy storage devices, *New J. Chem.*, 2020, **44**(18), 7369–7375.

55 V. L. Kuznetsov, A. L. Chuvilin, Y. V. Butenko, I. Y. Mal'kov and V. M. Titov, Onion-like carbon from ultra-disperse diamond, *Chem. Phys. Lett.*, 1994, **222**(4), 343–348.

56 X. Xu, G. Wang, G. Wan, S. Shi, C. Hao, Y. Tang and G. Wang, Magnetic Ni/graphene connected with conductive carbon nano-onions or nanotubes by atomic layer deposition for lightweight and low-frequency microwave absorption, *J. Chem. Eng.*, 2020, **382**, 122980.

57 M. Zeiger, N. Jäckel, M. Aslan, D. Weingarth and V. Presser, Understanding structure and porosity of nanodiamond-derived carbon onions, *Carbon*, 2015, **84**, 584–598.

58 T.-J. Park, S. Banerjee, T. Hemraj-Benny and S. S. Wong, Purification strategies and purity visualization techniques for single-walled carbon nanotubes, *J. Mater. Chem.*, 2006, **16**(2), 141–154.

59 V. Dhand, M. Yadav, S. H. Kim and K. Y. Rhee, A comprehensive review on the prospects of multi-functional carbon nano onions as an effective, high-performance energy storage material, *Carbon*, 2021, **175**, 534–575.

60 M. Zeiger, N. Jäckel, D. Weingarth and V. Presser, Vacuum or flowing argon: what is the best synthesis atmosphere for nanodiamond-derived carbon onions for supercapacitor electrodes?, *Carbon*, 2015, **94**, 507–517.

61 Z. Feng, Y. Lin, C. Tian, H. Hu and D. Su, Combined study of the ground and excited states in the transformation of nanodiamonds into carbon onions by electron energy-loss spectroscopy, *Sci. Rep.*, 2019, **9**(1), 3784.

62 C. He, N. Zhao, X. Du, C. Shi, J. Ding, J. Li and Y. Li, Low-temperature synthesis of carbon onions by chemical vapor deposition using a nickel catalyst supported on aluminum, *Scr. Mater.*, 2006, **54**(4), 689–693.

63 Y. M. Manawi, Ihsanullah, A. Samara, T. Al-Ansari and M. A. Atieh, A Review of Carbon Nanomaterials' Synthesis via the Chemical Vapor Deposition (CVD) Method, *Materials*, 2018, **11**(5), 822.

64 C. Zhang, J. Li, C. Shi, E. Liu, X. Du, W. Feng and N. Zhao, The efficient synthesis of carbon nano-onions using chemical vapor deposition on an unsupported Ni–Fe alloy catalyst, *Carbon*, 2011, **49**(4), 1151–1158.

65 D. Medranda, J. Borowiec, X. Zhang, S. Wang, K. Yan, J. Zhang, Y. He, S. Ivaturi and F. S. Boi, Ferromagnetically filled carbon nano-onions: the key role of sulfur in dimensional, structural and electric control, *R. Soc. Open Sci.*, 2018, **5**(1), 170981.

66 N. Sano, H. Wang, I. Alexandrou, M. Chhowalla, K. Teo, G. Amaratunga and K. Iimura, Properties of carbon onions produced by an arc discharge in water, *J. Appl. Phys.*, 2002, **92**(5), 2783–2788.

67 R. Borgohain, J. Yang, J. P. Selegue and D. Y. Kim, Controlled synthesis, efficient purification, and electrochemical characterization of arc-discharge carbon nano-onions, *Carbon*, 2014, **66**, 272–284.

68 F. Alessandro, A. Scarcello, M. D. B. Valverde, D. C. C. Fiallos, S. M. Osman, A. Cupolillo, M. Arias, O. A. De Fuentes, G. De Luca and A. Aloise, Selective synthesis of turbostratic polyhedral carbon nano-onions by arc discharge in water, *Nanotechnology*, 2018, **29**(32), 325601.

69 C. Ruan and Y. Lian, Purification of carbon nano-onions fabricated by arc discharge, *Fullerenes, Nanotub. Carbon Nanostruct.*, 2015, **23**(6), 488–493.

70 C. Ruan, J. Leng and Y. Lian, Electrochemical Performance of Carbon Onions Fabricated by Electric Arc-Discharge Method, *Electroanalysis*, 2016, **28**(1), 145–150.

71 D. Mohapatra, S. Badrayyana and S. Parida, Facile wick-and-oil flame synthesis of high-quality hydrophilic onion-like carbon nanoparticles, *Mater. Chem. Phys.*, 2016, **174**, 112–119.

72 G. S. Das, R. Panigrahi, S. Ghosh and K. M. Tripathi, Waste frying oil derived carbon nano-onions as a cost-effective cathode material for high-voltage zinc-ion hybrid supercapacitors, *Mater. Today Sustain.*, 2024, **25**, 100656.

73 P. Kumari, K. M. Tripathi, K. Awasthi and R. Gupta, Biomass-derived carbon nano-onions for the effective elimination of organic pollutants and oils from water, *Environ. Sci. Pollut. Res.*, 2023, **30**(27), 71048–71062.

74 W. Sun, X. Zhang, H.-R. Jia, Y.-X. Zhu, Y. Guo, G. Gao, Y.-H. Li and F.-G. Wu, Water-Dispersible Candle Soot–Derived Carbon Nano-Onion Clusters for Imaging-Guided Photothermal Cancer Therapy, *Small*, 2019, **15**(11), 1804575.

75 M. Zhou, Q. Li, S. Zhong, J. Chen, H. Lin and X.-L. Wu, Facile large scale fabrication of magnetic carbon nano-onions for efficient removal of bisphenol A, *Mater. Chem. Phys.*, 2017, **198**, 186–192.

76 K. M. Tripathi, T. S. Tran, Y. J. Kim and T. Kim, Green Fluorescent Onion-Like Carbon Nanoparticles from Flaxseed Oil for Visible Light Induced Photocatalytic Applications and Label-Free Detection of Al(III) Ions, *ACS Sustain. Chem. Eng.*, 2017, **5**(5), 3982–3992.

77 D. Patel, K. M. Tripathi and R. K. Sonwani, Waste-Derived Carbon Nano-Onions for the Removal of Organic Dye from Wastewater and Phytotoxicity Studies, *ACS Omega*, 2024, **9**(28), 30834–30845.

78 P. Kumari, K. M. Tripathi, K. Awasthi and R. Gupta, Cost-Effective and Ecologically Sustainable Carbon Nano-Onions for Antibiotic Removal from Wastewater, *Ind. Eng. Chem. Res.*, 2023, **62**(35), 13837–13847.

79 P. Kumari, K. M. Tripathi, K. Awasthi and R. Gupta, Ecologically viable carbon nano-onions for the efficient removal of methyl orange azo dye and its environmental assessment, *Environ. Sci.:Water Res. Technol.*, 2024, **10**(8), 1856–1870.

80 Y. Zhang, W. Zhang, K. Yang, Y. Yang, J. Jia, Y. Liang and L. Guo, Carbon Nano-Onions (CNOs)/TiO2 Composite Preparation and Its Photocatalytic Performance under Visible Light Irradiation, *Environ. Eng.*, 2020, **146**(4), 04020009.

81 W. Zhang, Y. Zhang, K. Yang, Y. Yang, J. Jia and L. Guo, Photocatalytic Performance of SiO2/CNOs/TiO2 to Accelerate the Degradation of Rhodamine B under Visible Light, *Nanomaterials*, 2019, **11**(5), 822.
82 W. Zhang, J. Wang, Y. Yang, Y. Liang and Z. Gao, Novel magnetically retrievable Bi2WO6/magnetic carbon nano-onions composite with enhanced photoactivity under visible light, *J. Colloid Interface Sci.*, 2018, **531**, 502–512.
83 L. Han, P. Zhang, L. Li, S. Lu, B. Su, X. An and Z. Lei, Nitrogen-containing carbon nano-onions-like and graphene-like materials derived from biomass and the adsorption and visible photocatalytic performance, *Appl. Surf. Sci.*, 2021, **543**, 148752.
84 L. Shi, F. Wang, J. Zhang and J. Sun, Onion-like carbon modified porous graphitic carbon nitride with excellent photocatalytic activities under visible light, *Ceram. Int.*, 2016, **42**(16), 18116–18123.
85 S. J. Park, G. S. Das, F. Schütt, R. Adelung, Y. K. Mishra, K. M. Tripathi and T. Kim, Visible-light photocatalysis by carbon-nano-onion-functionalized ZnO tetrapods: degradation of 2,4-dinitrophenol and a plant-model-based ecological assessment, *NPG Asia Mater.*, 2019, **11**(1), 8.
86 A. Inoue, T. Seto and Y. Otani, Onion-like carbon nanoparticles generated by multiple laser irradiations on laser-ablated particles, *Carbon*, 2012, **50**(3), 1116–1122.
87 O. Mykhailiv, H. Zubyk and M. E. Plonska-Brzezinska, Carbon nano-onions: unique carbon nanostructures with fascinating properties and their potential applications, *Inorg. Chim. Acta*, 2017, **468**, 49–66.
88 K. Thakur and B. Kandasubramanian, Graphene and Graphene Oxide-Based Composites for Removal of Organic Pollutants: A Review, *J. Chem. Eng. Data*, 2019, **64**(3), 833–867.
89 S. Taghipour, S. M. Hosseini and B. Ataie-Ashtiani, Engineering nanomaterials for water and wastewater treatment: review of classifications, properties and applications, *New J. Chem.*, 2019, **43**(21), 7902–7927.
90 R. P. Sah, B. Choudhury and R. K. Das, A review on adsorption cooling systems with silica gel and carbon as adsorbents, *Renew. Sustain. Energy Rev.*, 2015, **45**, 123–134.
91 T. Ma, P. R. Chang, P. Zheng, F. Zhao and X. Ma, Fabrication of ultra-light graphene-based gels and their adsorption of methylene blue, *Chem. Eng. J.*, 2014, **240**, 595–600.
92 T. J. Sahetya, F. Dixit and K. Balasubramanian, Waste citrus fruit peels for removal of Hg(II) ions, *Desalination Water Treat.*, 2015, **53**(5), 1404–1416.
93 P. H. R., Kapillarchemie, Eine Darstellung der Chemie der Kolloide und verwandter Gebiete, *Nature*, 1911, **85**(2156), 534–535.
94 I. Langmuir, The adsorption of gases on plane surfaces of glass, mica and platinum, *J. Am. Chem. Soc.*, 1918, **40**(9), 1361–1403.
95 A. Chowdhury, S. Kumari, A. A. Khan, M. R. Chandra and S. Hussain, Activated carbon loaded with Ni-Co-S nanoparticle for superior adsorption capacity of antibiotics and dye from wastewater: kinetics and isotherms, *Colloids Surf., A*, 2021, **611**, 125868.
96 R. A. Venkatesan and M. Balachandran, Novel carbon nano-onions from paraffinum liquidum for rapid and efficient removal of industrial dye from wastewater, *Environ. Sci. Pollut. Res.*, 2020, **27**(35), 43845–43864.
97 D. Saini, Gunture, J. Kaushik, R. Aggarwal, K. M. Tripathi and S. K. Sonkar, Carbon Nanomaterials Derived from Black Carbon Soot: A Review of Materials and Applications, *ACS Appl. Nano Mater.*, 2021, **4**(12), 12825–12844.
98 X. An and J. C. Yu, Graphene-based photocatalytic composites, *RSC Adv.*, 2011, **1**(8), 1426–1434.
99 S. Chowdhury and R. Balasubramanian, Graphene/semiconductor nanocomposites (GSNs) for heterogeneous photocatalytic decolorization of wastewaters contaminated with synthetic dyes: a review, *Appl. Catal., B*, 2014, **160–161**, 307–324.
100 U. G. Akpan and B. H. Hameed, Parameters affecting the photocatalytic degradation of dyes using TiO2-based photocatalysts: a review, *J. Hazard. Mater.*, 2009, **170**(2), 520–529.
101 S. Ahmed, M. G. Rasul, R. Brown and M. A. Hashib, Influence of parameters on the heterogeneous photocatalytic degradation of pesticides and phenolic contaminants in wastewater: a short review, *J. Environ. Manage.*, 2011, **92**(3), 311–330.
102 M. A. Rauf, M. A. Meetani and S. Hisaindee, An overview on the photocatalytic degradation of azo dyes in the presence of TiO2 doped with selective transition metals, *Desalination*, 2011, **276**(1), 13–27.
103 A. R. Khataee and M. B. Kasiri, Photocatalytic degradation of organic dyes in the presence of nanostructured titanium dioxide: influence of the chemical structure of dyes, *J. Mol. Catal. A:Chem.*, 2010, **328**(1), 8–26.
104 W. Zhang, J. Wang, Y. Yang, Y. Liang and Z. Gao, Novel magnetically retrievable Bi2WO6/magnetic carbon nano-onions composite with enhanced photoactivity under visible light, *J. Colloid Interface Sci.*, 2018, **531**, 502–512.
105 Q. Li, B. Guo, J. Yu, J. Ran, B. Zhang, H. Yan and J. R. Gong, Highly Efficient Visible-Light-Driven Photocatalytic Hydrogen Production of CdS-Cluster-Decorated Graphene Nanosheets, *J. Am. Chem. Soc.*, 2011, **133**(28), 10878–10884.
106 H. Asati, R. Mondal and K. M. Tripathi, Ultra-fast microwave catalytic degradation of multiple dyes by waste derived carbon nano onions, *Mater. Today Chem.*, 2024, **26**, 100724.
107 C. G. Renda, L. A. Goulart, C. H. M. Fernandes, L. H. Mascaro, J. M. de Aquino and R. Bertholdo, Novel onion-like carbon structures modified with iron oxide as photocatalysts for the degradation of persistent pollutants, *J. Environ. Chem. Eng.*, 2021, **9**(1), 104934.
108 P. Kumari, K. M. Tripathi, K. Awasthi and R. Gupta, Sustainable carbon nano-onions as an adsorbent for the efficient removal of oxo-anions, *Environ. Sci. Pollut. Res.*, 2023, **30**(6), 15480–15489.

109 P. Kumari, K. M. Tripathi, K. Awasthi and R. Gupta, Adsorptive Removal of Nitrophenols from Water by Biomass-Derived Carbon Nano-Onions, *Ind. Eng. Chem. Res.*, 2023, **62**(46), 19801–19812.

110 Gunture, J. Kaushik, A. K. Garg, D. Saini, P. Khare and S. K. Sonkar, Pollutant Diesel Soot Derived Onion-like Nanocarbons for the Adsorption of Organic Dyes and Environmental Assessment of Treated Wastewater, *Ind. Eng. Chem. Res.*, 2020, **59**(26), 12065–12074.

111 Y. C. López, F. J. Chao-Mujica, L. M. García-Rodríguez, O. L. Perez-Guevara, M. Antuch, E. Reguera, L. F. Desdin-García and L. Garcia-Hernández, Neutral red dye adsorption on carbon nano-onions: viability assay interference and adduct characterisation, *Adv. Nat. Sci. Nanosci. Nanotechnol.*, 2022, **13**(4), 045001.

112 C. Sakulthaew, C. Chokejaroenrat, A. Poapolathep, T. Satapanajaru and S. Poapolathep, Hexavalent chromium adsorption from aqueous solution using carbon nano-onions (CNOs), *Chemosphere*, 2017, **184**, 1168–1174.

113 L. Han, P. Zhang, L. Li, S. Lu, B. Su, X. An and Z. Lei, Nitrogen-containing carbon nano-onions-like and graphene-like materials derived from biomass and the adsorption and visible photocatalytic performance, *Appl. Surf. Sci.*, 2021, **543**, 148752.

114 S. Kar, K. Bramhaiah, N. S. John and S. Bhattacharyya, Insight into the Multistate Emissive N, P-doped Carbon Nano-Onions: Emerging Visible-Light Absorption for Photocatalysis, *Chem.–Asian J.*, 2021, **16**(9), 1138–1149.

115 T. D. Ntuli, L. L. Sikeyi, F. Dziike, N. J. Coville, E. N. Nxumalo and M. S. Maubane-Nkadimeng, Improved Adsorption and Photocatalytic Degradation of Methyl Orange by Onion-like Nanocarbon/TiO2 Nanocomposites, *Appl. Sci.*, 2023, **13**(8), 5125.

116 C. G. Renda, L. A. Goulart, C. H. M. Fernandes, L. H. Mascaro, J. M. de Aquino and R. Bertholdo, Novel onion-like carbon structures modified with iron oxide as photocatalysts for the degradation of persistent pollutants, *J. Environ. Chem. Eng.*, 2021, **9**(1), 104934.